

# Possible Solution to the Triple Alpha Fine-Tuning Problem: Spallation Reactions during Planet Formation

Fred C Adams<sup>a,b</sup>

<sup>a</sup>*Leinweber Center for Theoretical Physics, Physics Department, University of Michigan, Ann Arbor, MI 48109*

<sup>b</sup>*Astronomy Department, University of Michigan, Ann Arbor, MI 48109*

---

## Abstract

Carbon is produced during the helium burning phase of sufficiently massive stars through the triple alpha process. The  $0^+$  energy level of the carbon nucleus allows for resonant nuclear reactions, which act to greatly increase the carbon yields compared to the non-resonant case. Many authors have argued that small changes to the energy level of this resonance would lead to a significantly lower carbon abundance in the universe, and this sensitivity is often considered an example of fine-tuning. By considering spallation reactions occurring during the process of planet formation, this paper presents a partial solution to this triple alpha fine-tuning problem. Young stellar objects generate substantial luminosities of particle radiation (cosmic rays) that can drive nuclear reactions through spallation. If the standard triple alpha process is inoperative, stars tend to synthesize oxygen (and other alpha elements) rather than carbon. Cosmic rays can interact with oxygen nuclei to produce carbon while planets are forming. The resulting carbon abundances are significant, but much smaller than those observed in our universe. However, for a range of conditions — as delineated herein — spallation reactions can result in carbon-to-oxygen ratios roughly comparable to those found on Earth and thereby obviate the triple alpha fine-tuning problem.

*Keywords:* Fine-tuning; Multiverse; Nucleosynthesis

---

## 1. Introduction

The laws of physics, as realized in our universe, are characterized by a collection of fundamental constants that set the strength of the forces and the masses of particles; additional cosmological quantities specify the inventory of the universe [1, 2]. All of these parameters have the proper values to allow for a long-lived universe that can develop a range of cosmic structures, including galaxies, stars, planets, complex nuclei, and even life. A great deal of previous work has considered the possibility that the fundamental constants could have different values, and has explored the degree to which they can vary and still allow the universe to be habitable [3, 4, 5, 6, 7, 8, 9]. Within this enterprise, an important issue is the production of carbon, an essential ingredient for the development of life, at least in terrestrial forms. Variations in the fundamental constants can lead to corresponding variations in the resonance levels of the carbon nucleus, and can significantly change the carbon production rate during stellar nucleosynthesis. The resulting carbon abundance depends rather sensitively on the carbon resonance structure and hence on the underlying fundamental constants. This sensitivity is often cited as an example of fine-tuning, where small changes to the fundamental constants could lead to large changes in carbon production and lead to a lifeless universe. This paper explores an alternate channel of carbon production through spallation reactions that take place during the planet formation process and thus offers a way to avoid the triple alpha fine-tuning problem.

Carbon is synthesized in stars during their helium burning phases and occurs through the triple alpha process [10, 11]. The expected reaction, where two  ${}^4\text{He}$  nuclei are forged into a  ${}^8\text{Be}$  nucleus, is compromised because the  ${}^8\text{Be}$  nucleus is unstable, with a half-life of only  $t_{1/2} \sim 10^{-16}$  sec. Even with this short half-life, however, the stellar core builds up a small transient population of  ${}^8\text{Be}$ , which can then interact with additional alpha particles to produce carbon [12]. The latter reaction occurs rapidly enough to account for the carbon inventory of our universe, but requires a resonance in the carbon nucleus [13], where the resonance energy is 7.644 MeV [14], and corresponds to a  $0^+$  nuclear state of the carbon nucleus. If the energy level of the resonance were higher (lower), then the reaction rate could be slower (faster), resulting in different carbon yields.

Previous work has explored the sensitivity of carbon production to the specific value of the carbon resonance energy level. These studies show that the energy level of the resonance is sensitive to the values of the fundamental

constants [15, 16] and that the carbon yields in stars are sensitive to the value of the resonance [17, 18, 19]. If the resonance energy is higher, with  $(\Delta E_R) > 0$ , then carbon yields from massive stars decrease. In contrast, lower resonance levels with  $(\Delta E_R) < 0$  lead to increased carbon production. The range of resonance energy that allows for net carbon production is approximately  $-300 \text{ keV} \leq (\Delta E_R) \leq 500 \text{ keV}$ , or a total span of  $\sim 800 \text{ keV}$  [19]. This range should be compared to the spacing of energy levels in the carbon nucleus, about  $3 \text{ MeV}$ , which implies roughly a one in four chance of the resonance energy falling in the proper range to allow for carbon production. As another point of comparison, the  ${}^8\text{Be}$  nucleus only fails to be stable by  $92 \text{ keV}$ . As a result, the changes to the energy levels of nuclei required to compromise the triple alpha process are almost an order of magnitude larger than the changes needed to make  ${}^8\text{Be}$  stable. The latter possibility allows for carbon production without any need for the triple alpha process [20].

The above discussion applies to the *net* amount of carbon produced in stars. For the parameter choices that lead to low carbon yields, the stars still process alpha particles into carbon. The issue is that the nuclear burning temperature required for carbon production becomes large enough that newly synthesized carbon is promptly processed into oxygen (e.g., through the reaction  ${}^{12}\text{C} + {}^4\text{He} \rightarrow {}^{16}\text{O}$ ), so that relatively little carbon remains. For even more extreme parameter choices, much of the oxygen can be processed into larger alpha elements such as neon, magnesium, and silicon. As a result, when stars fail to produce substantial amounts of carbon, they leave behind oxygen and other alpha elements instead. These nuclei can be broken down to produce carbon through spallation reactions.

Note that this paper implicitly considers variations in the energy levels of carbon of order  $100$  to  $500 \text{ keV}$ . Although the binding energies of carbon, oxygen, and other alpha elements are expected to also change by roughly comparable increments, such changes are small in relative terms. Recall that the binding energy of carbon is about  $92 \text{ MeV}$ , and that for oxygen is about  $124 \text{ MeV}$  [10]. As a result, changes to the binding energies are small, even though large changes to the carbon production rates can be realized.

By considering spallation reactions that convert oxygen into carbon during the process of planet formation, this paper constructs an alternate mechanism to circumvent the triple alpha fine-tuning problem. Planets form in the circumstellar disks associated with young stellar objects during the first  $\sim 1 - 10 \text{ Myr}$  of evolution. During this time span, the stellar hosts produce copious amounts of particle radiation — cosmic rays — which have the

potential to change the nuclear composition of the planet-forming material through spallation. In the model explored here, strong magnetic fields couple to the disk at radii  $r \sim r_X \sim 0.1$  AU, where reconnection events lead to particle acceleration and large fluxes of cosmic rays (Section 2). This particle radiation can drive spallation reactions that convert some fraction of the oxygen nuclei into carbon (Section 3). Because the cosmic rays originate near the inner edge of the disk, planets forming with shorter orbital periods tend to have higher carbon abundances. For small stars, planets in the habitable zone can have carbon to oxygen ratios comparable to that of Earth (Section 4). As summarized in Section 5, this scenario allows for the development of potentially habitable planets, even in universes where the triple alpha process cannot produce high enough carbon yields through stellar nucleosynthesis.

## 2. Production of Particle Radiation during Early Stellar Evolution

During their early formative phases, young stars are accompanied by circumstellar disks that provide the initial conditions for the planet formation process. These disks are truncated near the host star due to the strong magnetic fields generated within the star. The magnetic truncation radius  $r_X$  is determined by the balance between the inward pressure due to mass accretion through the disk and the outward pressure due to the fields, and can be written in the form

$$r_X = \eta \left( \frac{B_*^4 R_*^{12}}{GM_* \dot{M}^2} \right)^{1/7}, \quad (1)$$

where  $\dot{M}$  is the mass accretion rate and  $B_*$  is the field strength on the stellar surface. Other parameters include the stellar radius  $R_*$  and the stellar mass  $M_*$ . Finally,  $\eta$  is a dimensionless parameter that is expected to be of order unity, and its value varies with the model details [21, 22]. For typical pre-main-sequence stars, surface field strengths fall in the range  $B_* \approx 1 - 2$  kilogauss, so that truncation radii  $r_X \sim 0.1$  AU (note that all of the physical quantities appearing in equation [1] have been measured for a large number of pre-main-sequence stars [23]).

In the astrophysical model under consideration [24, 25], particle acceleration occurs due to magnetic reconnection events that take place near the truncation radius of equation (1). The strong magnetic field lines tend to make the star co-rotate with the inner edge of the disk (at  $r_X$ ), but fluctuations in the mass accretion rate, the magnetic field strength, and other

parameters require the field lines to continually adjust through reconnection events. This magnetic activity, in turn, leads to particle acceleration. This process is essentially a scaled-up version of the mechanism that produces cosmic radiation in the Sun [26]. The luminosity  $L_p$  in energetic particles is expected to be comparable to, but somewhat less than, the luminosity  $L_X$  emitted in X-rays [27]. The latter luminosity is observed to be a substantial fraction of the photon luminosity  $L_*$ , with both temporal and source-to-source variations [28, 29]. As a result, the power contributions from young stellar objects are ordered according to the relation

$$L_p \sim 10^{-1} L_X \sim 10^{-4} L_*. \quad (2)$$

Note that pre-main-sequence stars are brighter than their main sequence counterparts, and that low mass stars evolve more slowly than larger stars during PMS contraction. As a result, the typical stellar luminosity is given by  $L_* \sim 1L_\odot$  during the epoch of planet formation (stellar ages  $t \lesssim 10$  Myr).

Cosmic rays generally have a power-law energy distribution [30, 31], which can be written in the form

$$\frac{dN}{dE} = f(E) = \frac{p-1}{E_0} \left( \frac{E_0}{E} \right)^p, \quad (3)$$

where the distribution is normalized over the range  $E_0 \leq E \leq \infty$ . For cosmic radiation generated in the Sun through gradual flares, the power-law index  $p \approx 2.7$  [32]. For particle radiation generated through impulsive flares, the distribution is steeper with  $p \approx 3.5$ . For the sake of definiteness, we use  $p = 3$  for the estimates of this paper (for completeness, note that the distribution for galactic cosmic rays has energy dependence  $\sim E^{-2.7}$  at high energies, which is roughly similar). The luminosity relations of equation (2) correspond to cosmic rays with energies  $E \geq E_0 = 10$  MeV. As outlined below, the energy threshold  $E_{th}$  for the nuclear reactions of interest is comparable to, but somewhat larger than, the scale  $E_0$ . For a given energy spectrum, the number of cosmic rays produced per unit time  $\dot{\mathcal{N}}_{CR}$  with energies  $E \geq E_{th}$  is related to the luminosity  $L_p$  according to

$$\dot{\mathcal{N}}_{CR} = \frac{p-2}{p-1} \frac{L_p}{E_0} \left( \frac{E_0}{E_{th}} \right)^{p-1} = \frac{L_p}{2E_0} \left( \frac{E_0}{E_{th}} \right)^2, \quad (4)$$

where the final equality assumes the index  $p = 3$ . Here,  $L_p$  is the total luminosity in cosmic rays over the energy range  $E \geq E_0$ , so that the factor

$(E_0/E_{th})^2$  corrects for the inclusion of only those particles with energy  $E \geq E_{th} \geq E_0$ .

In this scenario, the cosmic radiation is generated within an annulus in the disk roughly centered on the truncation radius  $r_X$  from equation (1). As a result, the number flux (fluence) of cosmic rays that is generated with energy  $E > E_{th}$  is given by

$$\Phi_{CR} \approx \frac{\dot{N}_{CR}}{\pi r_X^2} = \frac{L_p E_0}{2\pi r_X^2 E_{th}^2} \approx 2 \times 10^9 \left( \frac{E_0}{E_{th}} \right)^2 \text{ cm}^{-2} \text{ s}^{-1}, \quad (5)$$

where the numerical estimate uses  $E_0 = 10 \text{ MeV}$ ,  $L_p = 10^{-4} L_\odot$ , and  $r_X = 0.1 \text{ AU}$ .

Equation (5) specifies the number flux in the vicinity of the truncation radius  $r \sim r_X$ . The subsequent propagation of the particles from their point of origin is complicated. Since the magnetic field lines are continually wrapped up by the shear flow from the disk, and then reconnected, the corresponding field structure is expected to be complex and chaotic in the region where the cosmic rays are accelerated.

In this setting, the disk scale height  $h$  provides an important length scale in the problem, where  $h \sim r_X/20$  (see, e.g., [24]). The cosmic rays propagate by moving along the field lines, with a typical length scale  $h$ , and perpendicular to the field lines, with typical length scale set by the magnetic gyroradius  $r_g = \gamma mc v/qB$ . For typical energy (10 MeV – 10 GeV) and field strength ( $B \sim 1 \text{ gauss}$ ),  $r_g \ll h$ , so that the particles are tied to the magnetic field and travel along the highly convoluted field lines. In the absence of attenuation, cosmic ray propagation can thus be modeled as a random walk with step length  $h$  (note that attenuation is considered in the following section). In order for cosmic rays to leave the annulus where they are generated, they must travel a total distance  $d \sim r_X = \sqrt{N}h$ , where  $N$  is the required number of steps. As a result, the cosmic rays must propagate across the disk scale height many times before escaping, i.e.,  $\mathcal{M} = (r_X/h)^2 \sim 400$ . The total distance traveled is given by  $\mathcal{M}h = r_X^2/h \sim 20r_X$ . With such a long path length, a large fraction of the cosmic rays will be absorbed within the annulus where they are generated.

### 3. Spallation of Oxygen to make Carbon in Circumstellar Disks

The current working scenario for rocky planet formation can be summarized as follows. The raw materials for planet formation begin in the form of

dust grains. In the interstellar medium, a substantial fraction of the metals (elements beyond helium) are locked up in these entities. Although they have a distribution of sizes, the grains begin with a typical size  $b_g \sim 0.1 - 1 \mu\text{m}$ . Within the circumstellar disks that form planets, the dust grains grow into larger bodies, sometimes known as pebbles, with sizes  $b_p \sim 0.1 - 1 \text{ cm}$ . The pebbles sink to the midplane of the disk, experience a streaming instability, and thereby produce rocky planetesimals with sizes  $b_R \sim 1 - 100 \text{ km}$  [33] (alternately, planetesimals can be produced through a gravitational instability [34]). These planetesimals subsequently accumulate into rocky terrestrial planets.

In our galaxy the original dust grains, and hence the rocks they grow into, are generally composed of both silicates and graphite, with admixtures of many other minerals [35]. For the case under consideration here, with little carbon produced in stars, the grains are expected to be primarily silicates and thus contain a large mass fraction of oxygen. For example, typical compounds found in solar system rocks include  $\text{SiO}_2$  and  $\text{Fe}_2\text{O}_3$  (see [36]).

If the rocky entities are exposed to a flux of cosmic radiation, then spallation can produce carbon through a number of possible reactions, e.g.,



along with many others. In this case, oxygen-16 represents the target nucleus. For common reaction products — such as carbon — the cross sections for such spallation reactions are generally of order  $\sigma_0 = 100 \text{ mb}$  [37, 38, 39, 40, 41]. For spallation reactions that convert oxygen to carbon, the data show that there is an effective threshold energy at  $E = E_{th} \approx 15 \text{ MeV}$ , where the cross section rises steeply as a function of energy, and then varies slowly for larger energies. For the estimates of this paper, we adopt the simple approximation where  $\sigma(E) = \sigma_0 = 100 \text{ mb} = 10^{-25} \text{ cm}^2$  for  $E \geq E_{th}$  and  $\sigma(E) = 0$  otherwise.

Carbon production is maximized if the target oxygen nuclei are exposed to the full flux of cosmic rays, i.e., in the optically thin limit. In practice, this condition holds if the rocky bodies are in the form of pebbles ( $b_p \sim 1 \text{ cm}$ ), whereas planetesimals ( $b_R \sim 1 - 100 \text{ km}$ ) are optically thick. On the other hand, if the bodies are too small ( $b_g \sim 1 \mu\text{m}$ ), they remain coupled to the gas and are swept into the star along with the gas in the accretion flow. We thus consider intermediate sizes. These centimeter-sized bodies are expected to be decoupled from the gas inside the truncation radius  $r < r_X$ , where the column density of the gas is low [24].

With the above specifications, the rate  $\Gamma$  at which a given target oxygen nucleus interacts to make carbon is given by

$$\Gamma = \Phi_{CR} \langle \sigma \rangle = \frac{L_p \sigma_0 E_0}{2\pi r_X^2 E_{th}^2}. \quad (7)$$

In the limit where the target nuclei are exposed to an unattenuated cosmic ray flux for an exposure time ( $\Delta t$ ), the time evolution of the carbon/oxygen inventory is given by

$$[C/O] = \frac{4 X_{C12}}{3 X_{O16}} = \exp[\Gamma(\Delta t)] - 1 \approx \Gamma(\Delta t) = \frac{L_p \sigma_0 E_0 (\Delta t)}{2\pi r_X^2 E_{th}^2} \sim 0.0025, \quad (8)$$

where  $[C/O]$  is the ratio of the number of carbon to oxygen nuclei and  $X_k$  is the corresponding mass fraction of the nuclear species (note that we also assume that carbon is the most common product of the spallation reactions). The final approximate equality holds in the expected limit where only a small fraction of the oxygen is converted. The numerical estimate assumes typical values for the parameters, i.e.,  $L_p = 10^{-4} L_\odot$ ,  $\sigma_0 = 100$  mb,  $E_0 = 10$  MeV,  $E_{th} = 15$  MeV,  $r_X = 0.1$  AU, and  $(\Delta t) = 1$  Myr.

Note that the above estimate only includes reactions for carbon production where oxygen nuclei are the target, but other targets are possible. In the scenario under consideration here, we are assuming that carbon is rare because most of the carbon produced in stars is immediately synthesized into oxygen. The expected oxygen abundance is thus given approximately by the combined mass fraction of carbon and oxygen in our solar system, or about  $\sim 2/3$  of the total mass fraction of metals [36]. The remaining  $\sim 1/3$  of the metal mass fraction provide additional targets for carbon production (as well as additional attenuation – see below). Since the corresponding reaction cross sections are lower, however, the correction for non-oxygen targets is expected to be modest. In any case, the neglect of alternate targets renders the estimates of this paper as lower limits.

The expected exposure time ( $\Delta t$ ) is subject to several constraints. Cosmic ray production occurs due to reconnection events taking place near the truncation radii of circumstellar disks, so the disk lifetime limits the exposure time (at least for the most energetic phases). Observed circumstellar disks have a distribution of lifetimes [42] that can be modeled as an exponential with half-life  $\sim 3$  Myr. As a result, only  $\sim 10\%$  of disks live as long as 10 Myr, which thus provides an approximate upper limit on ( $\Delta t$ ). As outlined below,

another constraint arises from the growth of the rocky material containing the oxygen targets. While the rocks are small, they are exposed to the full flux of cosmic rays, but shielding occurs once the rocks have grown larger than  $b \sim 1 - 10$  cm. The time at which rocky bodies cross this size threshold, typically a few Myr [43], provides another constraint on the effective exposure time. Calculations that explain the observed/inferred abundances of short lived radioactive nuclei in our solar system lead to similar time scale estimates [44]. In order for spallation to simultaneously produce the correct isotopic ratios for  $^{26}\text{Al}/^{27}\text{Al}$ ,  $^{41}\text{Ca}/^{40}\text{Ca}$ ,  $^{53}\text{Mn}/^{55}\text{Mn}$ , and  $^{92}\text{Nb}/^{92}\text{Nb}$ , the irradiation time must be of order  $\sim 1$  Myr (see also [24, 25]).

Since the target nuclei of interest tend to be locked up in rocky bodies, maximal exposure occurs only for sufficiently small entities. When cosmic rays enter rock, they lose energy primarily through electromagnetic interactions with electrons, rather than through nuclear reactions. For example, cosmic rays with energy  $E = 10$  MeV lose their energy after passing through a column density of only  $\Sigma_s \sim 0.3$  g cm $^{-2}$  [45, 46], with larger stopping columns for particles of higher energy. In addition to energy loss, the propagation of cosmic rays through rock is complicated by the emission of secondary particles, such as neutrons and electrons, which can propagate longer distances (although their impact is small in the present application). As a result, one must consider the full energy distribution of cosmic rays and perform detailed simulations of the process. For example, for the case of solar cosmic rays impinging on the Martian surface, the isotope production rate for carbon decreases with depth  $z$  with an nearly exponential fall-off [46]. Motivated by this finding we write the production rate in the approximate form

$$\gamma = \gamma_0 \exp[-z/\zeta], \quad (9)$$

where we expect the effective scale height  $\zeta \sim 1$  cm [45, 46] (and where this approximation is valid for solar cosmic rays). The corresponding rate coefficient  $\gamma_0$  is calculated for an incident flux of solar cosmic rays in the energy range  $E \geq 1$  MeV. If we rescale the coefficient to include only cosmic rays with energy  $E \geq E_0 = 10$  MeV, and define a benchmark number flux of protons  $\Phi_1 = 1$  cm $^{-2}$  s $^{-1}$ , then we find the value  $\gamma_0 \approx 0.003(\Phi_{CR}/\Phi_1)$  atom cm $^{-3}$  s $^{-1}$ , where  $\Phi_{CR}$  is the number flux of cosmic rays with energy  $E \geq 10$  MeV. Using these results, let us consider a cosmic ray flux  $\Phi_{CR}$  incident on a slab of rocky material with thickness  $b$ . The rate at which oxygen nuclei

are converted into carbon is given by the expression

$$\Gamma_R = \left( \frac{16m_p\gamma_0}{\rho_R X_{O16}} \right) \frac{\zeta}{b} [1 - \exp(-b/\zeta)] , \quad (10)$$

where  $\rho_R = 2.5 \text{ g cm}^{-3}$  is the density of the rock. In the limit of small thickness  $b \ll \zeta$ , the function on the right approaches unity, and the rate becomes

$$\Gamma_R(b \ll \zeta) \approx (10^{-25} \text{ s}^{-1}) \left( \frac{\Phi_{CR}}{\Phi_1} \right) . \quad (11)$$

This rate  $\Gamma_R(b \ll \zeta)$  can be compared to the optically thin rate  $\Gamma = \langle \sigma \rangle \Phi_{CR}$  from equation (7). The rates are comparable in this limit, as expected. For completeness, note that the optically thick rate from equation (10) in the optically thin limit (11) is equal to the optically thin rate from equation (7) for a specific choice of oxygen abundance (i.e., the rate coefficient  $\gamma_0$  depends on  $X_{O16}$ ). In any case, rocky bodies with size  $b \ll \zeta$  can be treated using the optically thin expression. As a working approximation, we assume that the net effect of rocky material aggregating into larger bodies of size  $b$  is to reduce the effective rate of converting oxygen into carbon by the factor  $\sim (\zeta/b)(1 - \exp[b/\zeta])$ . As a result, the largest rocks that remain optically thin have sizes less than about  $b \sim \zeta \sim 1 \text{ cm}$ .

For larger rocks,  $b > \zeta$ , only the outer layer is exposed to the cosmic ray flux. Within the region of disk where the cosmic rays are generated, strong but tangled magnetic fields confine the particle radiation, which must propagate diffusively. As a result, the cosmic radiation is expected to be nearly isotropic. For larger rocks, assuming spherical geometry, the fraction  $\mathcal{F}$  of their volume that will experience spallation reactions is given by

$$\mathcal{F} \approx 3 \left( \frac{\zeta}{b} \right) - 3 \left( \frac{\zeta}{b} \right)^2 + \left( \frac{\zeta}{b} \right)^3 \approx \frac{3\zeta}{b} , \quad (12)$$

where the final expression corresponds to the limit  $b \gg \zeta$ .

The discussion thus far assumes that the target oxygen nuclei, or rocky bodies that contain them, are exposed to the full flux of cosmic rays. If the total amount of solid material in the reconnection region is large enough, then the cosmic ray flux can be attenuated by background before reaching the rocks of interest. We can address this issue by estimating the optical depth of the background field of rocky material. Let the total mass  $M_s$  in solids be spread out over the reconnection region, which is an annulus with

radius comparable to the truncation radius  $r_X$ . The column density of solid material is thus given by

$$\Sigma_s \approx \frac{M_s}{\pi r_X^2}. \quad (13)$$

The solid material is primarily contained in rocky bodies, which can be considered as partially optically thick. We further consider the rocks to have a given radius  $b$ . As outlined above, the nuclei within the rocks are exposed to only a fraction  $\mathcal{F}(b)$  of the total cosmic ray flux, whereas the corresponding fraction  $[1 - \mathcal{F}(b)]$  is lost (primarily through electromagnetic interactions).<sup>1</sup> The optical depth of the reconnection region can then be written in the form

$$\tau_{back} \approx \frac{M_s}{\pi r_X^2} \frac{3}{4\rho b} [1 - \mathcal{F}(b)] \approx \frac{200}{(b/1 \text{ cm})} [1 - \mathcal{F}(b)], \quad (14)$$

where the numerical estimate uses benchmark values  $M_s = 1M_\oplus$  and  $r_X = 0.1 \text{ AU}$ . In the limit of large bodies  $b \gg \zeta$ , the fraction  $\mathcal{F} \rightarrow 0$ , so that all of the cosmic rays striking a given rocky body are lost. In this case, the optical depth  $\tau_{back}$  is determined by the surface (number) density of rocky bodies times their geometrical cross section. In the opposite limit of small rocks with  $b \ll \zeta$ , the fraction  $\mathcal{F} \rightarrow 1$  but  $1 - \mathcal{F} = \mathcal{O}(b/\zeta)$  so that the optical depth becomes independent of the rock size  $b$  (e.g., see [48]).

The optical depth  $\tau_{back}$  and the factor  $\mathcal{F}$  jointly determine the fraction  $f_{cr}$  of the total cosmic ray flux seen by the typical target nucleus. If we assume a simple one-dimensional geometry for cosmic ray propagation across the reconnection region, then the nuclei within the rocks are exposed to a fraction of the original cosmic ray flux given by

$$f_{cr} = \frac{1}{\tau_{back}} [1 - e^{-\tau_{back}}] \mathcal{F}(b). \quad (15)$$

The first factor takes into account the loss of cosmic rays due to the background sea of rocky bodies and the second factor represents the fraction of nuclei within a given rock that are exposed to cosmic rays.

The survival fraction  $f_{cr}$  depends on both the total amount of mass  $M_s$  in the reconnection region and the size  $b$  of the individual rocks. For solid masses  $M_s \ll 1M_\oplus$ , the optical depth  $\tau_{back} \ll 1$  and the survival fraction

---

<sup>1</sup>Note that the particles are still present, but they are slowed down below the energy threshold so that they are no longer useful for spallation reactions.

$f_{cr} = \mathcal{F}$ . If, in addition, the rocks are small so that  $b \lesssim 1$  cm, both  $f_{cr}$  and  $\mathcal{F}$  are of order unity so that the nuclei are exposed to nearly the full flux of cosmic rays. In this limit, the carbon-to-oxygen ratio evolves with time according to equation (8). In general, however, the interaction rate  $\Gamma$  (see also equation [7]) must be reduced by the factor  $f_{cr}$ . For example, in the case of large total mass  $M_s \gtrsim 1M_{\oplus}$ , the optical depth is expected to be large (of order  $\sim 100$ ), so that equation (15) reduces to  $f_{cr} \approx \mathcal{F}(b)/\tau_{back}$ . Since the rocks are (most likely) in the form of pebbles with  $b \sim 1$  cm, the fraction  $\mathcal{F} \sim 1$ , so that the reduction factor  $f_{cr} \sim 1/\tau_{back}$ .

For completeness, we note that cosmic rays can also lose energy through interactions with gas in the reconnection region. However, such losses are already incorporated into this treatment, since the cosmic ray luminosity  $L_p$ , as defined here, corresponds to those particles that are emitted, i.e., the particles that survive propagation over distances comparable to the inner disk size. Moreover, the column density of gas in the region  $r < r_X$  is expected to be small,  $\sim 10^{-4}$  g cm $^{-2}$ , based on soft X-ray observations of young stellar objects [24]. For the estimates of this paper, we take into account possible attenuation by considering smaller values of the original (net) cosmic ray luminosity  $L_p$ .

Figure 1 illustrates the possible time evolution of the carbon to oxygen ratio [C/O] for various levels of attenuation, corresponding to various total mass in solids in the reconnection region. If the rocky material resides in pebbles ( $b \sim 1$  cm) and experiences the full unattenuated flux of cosmic rays, then the [C/O] ratio evolves with exposure time according to equation (8), as shown by the solid black curve. The remaining curves show the time evolution of the [C/O] ratio for cases where the cosmic ray flux is attenuated, with the total optical depth given by  $\log_{10} \tau = 0.5$  (blue), 1.0 (cyan), 1.5 (magenta), and 2.0 (green). These optical depth values correspond to total masses in solid material of  $M_s/M_{\oplus} = 10^{-3/2}$ ,  $10^{-1}$ ,  $10^{-1/2}$ , and 1.0. The rocky material, which initially resides in small pebbles, eventually transitions into planetesimals with sizes  $R = 10 - 100$  km. At this point, the rate of transforming oxygen into carbon decreases abruptly by a factor of  $\sim 10^4 - 10^5$ . As a result, the [C/O] ratio effectively freezes out at the transition time, i.e., the transition time defines the effective exposure time.

We can summarize this scenario for carbon production as follows: The rocky material is expected to reside in the form of pebbles with size  $b \sim 1$  cm and the total mass in the reconnection region is comparable to that of a small rocky planet (so that  $M_s \sim 0.1 - 1M_{\oplus}$ ). Finally, the exposure time falls in

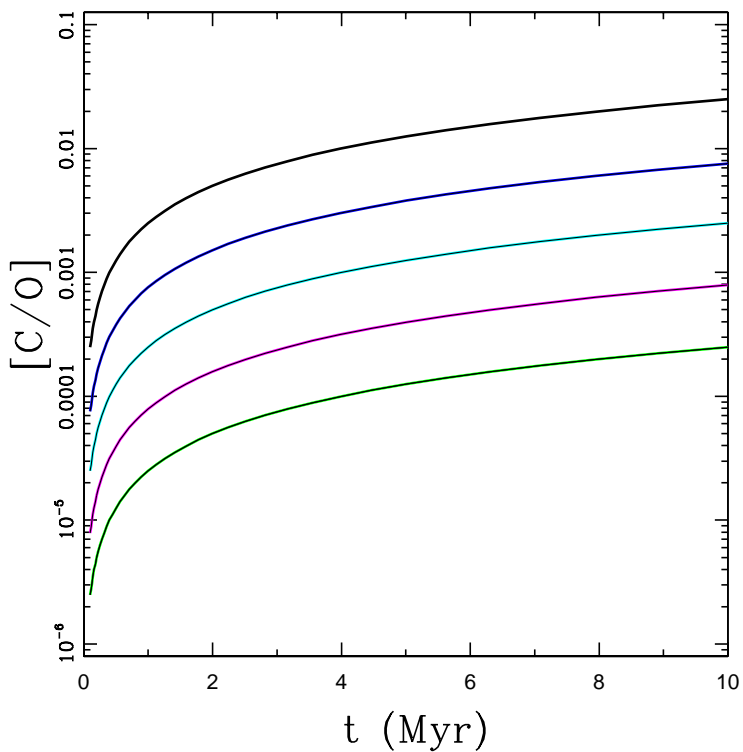


Figure 1: Time evolution of the carbon to oxygen ratio  $[C/O]$  for varying levels of attenuation. The upper black curve shows the maximum growth of  $[C/O]$  as a function of time for optically thin conditions and the full expected flux of cosmic rays. The remaining curves show the  $[C/O]$  ratio for total optical depths given by  $\tau_{back} \approx 3.16$  (blue), 10.0 (cyan), 31.5 (magenta), and 100 (green). For the expected case where the rocky material resides in pebbles ( $b \sim 1$  cm), these optical depths correspond to total mass in solids  $M_s/M_\oplus \approx 0.0316, 0.1, 0.316, \text{ and } 1.0$ , respectively.

the range  $(\Delta t) = 1 - 10$  Myr, consistent with observed disk lifetimes. Under these conditions, the optical depth of the background is large,  $\tau_{back} \gg 1$ , so that the survival fraction  $f_{cr} \propto \tau_{back}^{-1} \propto M_s^{-1}$ . Moreover, only a small fraction of the total number of oxygen nuclei will be processed into carbon. In this regime of parameter space, the carbon to oxygen ratio can be written in the form

$$[C/O] \approx 0.00025 \left( \frac{(\Delta t)}{10 \text{ Myr}} \right) \left( \frac{M_s}{M_\oplus} \right)^{-1}. \quad (16)$$

#### 4. Planet Formation and Habitable Zones

The previous sections show that cosmic rays are accelerated near the truncation radius  $r_X$ , are confined to nearby regions, and can interact with oxygen nuclei to make carbon. This section briefly considers the conditions necessary for the resulting carbon to be incorporated into a potentially habitable planet.

Even under the most favorable conditions, the carbon abundance is quite small, only a fraction of the total mass of the planet (which is made from the rocky raw material enriched via spallation). However, the Earth itself also has relatively little carbon, in contrast to its large abundance in both the Sun and the Galaxy. Even the carbon abundance for Earth's crust has been difficult to measure, with estimates of the carbon to oxygen ratio falling in the range  $[C/O] \approx 0.0002 - 0.01$  [49, 50, 51, 52, 53, 54]. Estimates for the bulk composition of Earth are more uncertain, but fall in a similar range. Finally, we note that oxygen makes up  $\sim 30\%$  of the Earth's mass, so the mass fraction of carbon is smaller than the carbon to oxygen ratio, say  $X_{C12} \sim 0.0001 - 0.003$ . Significantly, the  $[C/O]$  ratios that are produced through spallation reactions (Figure 1) can be comparable to (and under extreme conditions larger than) the values estimated for Earth. However, the largest  $[C/O]$  ratios only arise for relatively small total mass  $M_s$  in solids. To form planets with  $M_p = M_s = 1M_\oplus$  and an exposure time of 10 Myr, we find  $[C/O] \approx 0.0003$ , which is near the low end of the range inferred for Earth.

The most straightforward scenario is for the planet to form at the annulus centered on  $r_X$  where the cosmic rays are generated. In this case, the carbon to oxygen ratio in the rocky material will sample the values illustrated in Figure 1, i.e.,  $[C/O] \approx 10^{-5} - 10^{-2}$ . From this birth scenario, the resulting planetary orbit has a semimajor axis near  $a \sim r_X \sim 0.1$  AU. In order for the planet to receive the same stellar flux as Earth, the star must be less luminous

than the sun by a factor of 100, which corresponds to a main sequence star with mass  $M_* = 0.25M_\odot$ .

Figure 2 shows that rocky planets readily form near the location of the magnetic truncation radius where cosmic rays are generated. The blue histogram in the figure depicts the semimajor axes for a collection of exoplanets detected by the *Kepler* mission [55]. This sample includes the planets with inferred masses  $M_p \leq 7M_\oplus$  that are found in systems with three or more planets. Planets with masses below this threshold exhibit a primarily rocky composition, whereas larger planets tend to have extended atmospheres (although substantial variation exists). Only planets in multi-planet systems were used, as those tend to have nearly circular orbits and make up a uniform sample.<sup>2</sup> The green vertical lines show the locations of the magnetic truncation radii  $r_X$  for a collection of pre-main-sequence stars with measured magnetic field strengths [23]. The annulus where cosmic rays are accelerated through reconnection and flaring activity is expected to extend mostly inward from  $r_X$  [25]; to illustrate the extent of the enrichment region, the vertical cyan lines show locations corresponding to  $r_X/2$  for the same sample.

Note that the present-day locations of the planets (as shown in the figure) are not necessarily where they were formed. If rocky planets form at larger radial distances from their host stars, and subsequently migrate inward, then they would not be enriched in carbon through the mechanism considered here.

The stellar hosts for the planets shown in Figure 2 have masses in the range  $M_* \approx 0.10 - 1.35M_\odot$ , whereas the stellar masses for the  $r_X$  sample have  $M_* \approx 0.3 - 2 M_\odot$ . The stellar masses in both data sets thus span the same range and include the low mass stars of interest (where the habitable zones are roughly coincident with the disk truncation locations). Moreover, neither the planet masses  $M_p$  or the truncation radii  $r_X$  show any obvious trends with stellar mass.

Since we are interested in potentially habitable planets around smaller stars, it is important to note that M stars are generally more active than solar-type stars and are subject to intense flaring activity. Some authors have speculated that such energetic activity could be detrimental for planetary habitability. Although the conditions required for life remain unknown, this complication should be noted (see the discussion of [56] and references

---

<sup>2</sup>Keep in mind that for many planets the mass is inferred from measurement of the planetary radius, i.e., the mass is not directly determined.

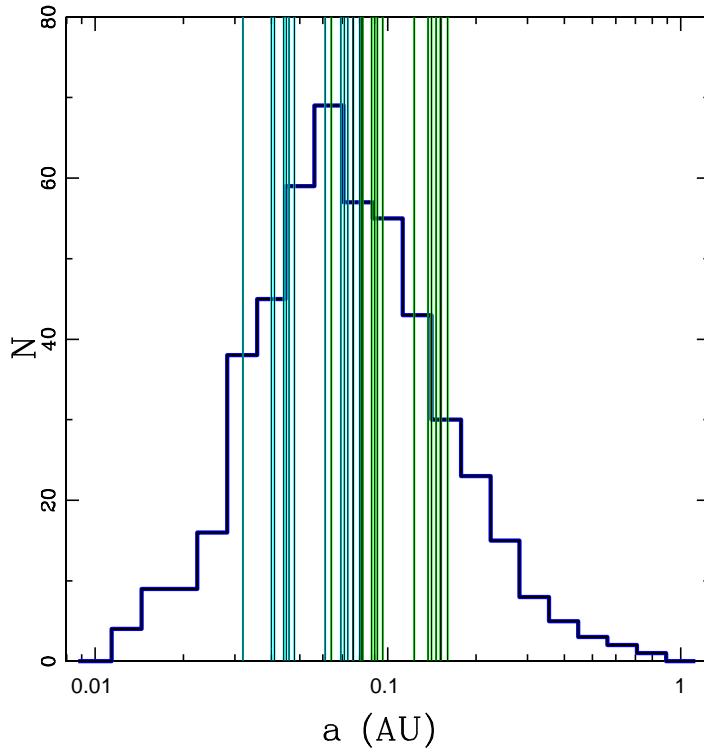


Figure 2: Histogram showing semimajor axes of observed rocky planets (thick blue curve) and the inferred positions of the magnetic truncation radius (vertical lines). The planet sample includes detected planets from the *Kepler* mission that have estimated masses  $M_p \leq 7M_\oplus$  and are found in systems containing 3 or more planets. The green lines show the locations of the magnetic truncation radii  $r_X$  for measured properties of pre-main-sequence stars [23] according to equation (1). The cyan lines show locations corresponding to half of the inferred values ( $r_X/2$ ). The region where cosmic rays are generated, as delineated by the collection of vertical lines, overlaps with the observed locations of rocky planets.

therein). On the other hand, the enhanced flaring activity of these small stars could result in enhanced spallation rates and somewhat larger carbon yields.

## 5. Conclusion

This paper presents a new possible solution to the triple alpha fine-tuning problem by considering how spallation changes the chemical composition of rocky planets forming in tight orbits around low-mass stars. If the fundamental constants of nature had different values, so that the Hoyle resonance in the carbon nucleus had a different energy level, then carbon production could be greatly reduced. This paper shows that even in universes that fail to produce carbon by stellar nucleosynthesis, some carbon is produced by spallation outside of stars. This argument can be summarized as follows:

If stars fail to produce substantial carbon yields, the nuclei are processed instead into oxygen and other alpha elements. These larger nuclei can be broken down into carbon by cosmic radiation through spallation reactions, thereby providing an alternate source of carbon.

Cosmic ray acceleration takes place near the magnetic truncation radius  $r_X$  in the disks associated with young stellar objects. Rocky planets readily form in this region, which is roughly located at  $a \sim r_X \sim 0.1$  AU (Figure 2). This region corresponds to the habitable zone for stellar hosts with masses  $M_* \sim 0.25M_\odot$ , which are the most common stars in our universe. As a result, the raw materials that make up this class of habitable planets are naturally irradiated by local (stellar) cosmic rays and are subject to spallation.

The amount of carbon produced depends on the timing of events that take place during the process of planet formation. For the expected cosmic ray luminosities, if the rocky material remains optically thin for a typical time scale of 1 Myr, then the resulting carbon to oxygen ratio  $[C/O] \sim 10^{-3}$ , comparable to the value inferred for Earth. However, this value is only realized for relatively small total masses  $M_s \ll M_\oplus$ . Longer exposure times lead to higher carbon yields, whereas larger masses  $M_s$  or larger rock sizes  $b$  lead to greater attenuation of the cosmic ray flux and hence smaller carbon yields (Figure 1). For example, if the total mass in solids in the reconnection region is comparable to Earth, then an exposure time of 10 Myr leads to  $[C/O] \approx 0.0003$ , near the low end of the range of inferred values for Earth.

The results of this work have a number of implications: Because spallation can produce carbon in universes where the triple alpha process is

inoperative, the fine tuning of the fundamental constants necessary for a viable universe is less severe than previously claimed. On the other hand, this spallation mechanism tends to produce only modest amounts of carbon,  $[C/O] \sim 10^{-4} - 10^{-3}$ , values roughly consistent with Earth abundances, but much smaller than that of the Sun or the universe as a whole. In addition, carbon production takes place within the habitable zones of smaller stars with masses  $M_* \sim 0.25 M_\odot$ . Although such hosts are the most common stars in our universe, the habitable zone for solar-type stars lies farther away from the cosmic ray source, so that direct analogs of our solar system would remain carbon poor. At the present time, we do not know exactly how much carbon is required for a planet, or a universe, to be habitable. Given the modest levels of carbon produced via spallation, however, it is likely that such universes would be somewhat less habitable than our own.

Another lesson from this consideration of spallation is that universes — including our own — have a number of possible channels to reach habitability. For example, a large number of different astrophysical sources contribute to the production of carbon and other elements, including supernova explosions, collisions of compact objects, red giant winds, spallation, and big bang nucleosynthesis (although the latter tends to make only light nuclei). If one channel of carbon production is unavailable, then astrophysics (often) provides alternate mechanisms. In the present context, spallation can produce carbon in other astrophysical settings, including the interstellar medium and on the surfaces of mature planets orbiting main sequence stars (as outlined in Appendix A).

Finally, we note that spallation from locally produced cosmic rays can have important implications for the chemical enrichment and early evolution of planets in our universe. In this context, carbon is already abundant, so any additional carbon produced via spallation is negligible. Spallation also produces short-lived radioactive nuclei, such as  $^{26}\text{Al}$ ,  $^{41}\text{Ca}$ ,  $^{53}\text{Mn}$ ,  $^{138}\text{La}$ ,  $^{10}\text{Be}$ , and others. These radionuclides provide important sources of heating and ionization during planet formation, and meteoritic evidence indicates that our solar system was enriched in these nuclei relative to cosmic abundances. A great deal of past work [24, 25, 57] has focused on radioactive enrichment mechanisms for solar system meteorites, at distances of order  $\sim$ few AU. Since many rocky planets form much closer to their host stars (e.g., Figure 2), they are expected to experience much greater levels of radioactive enrichment, which can influence the formation and properties of such systems [48].

**Acknowledgments:** We would like to thank Konstantin Batygin, Juliette Becker, George Fuller, Evan Grohs, Alex Howe, Jonathan Lunine, Martin Rees, and Chris Spalding for many useful discussions. We also thank an anonymous referee for many useful comments that improved the manuscript. This work was supported by the Leinweber Center for Theoretical Physics and by the University of Michigan.

## Appendix A. Alternate Scenarios for Carbon Production

As outlined in the main text, intense cosmic ray production is expected to continue only while circumstellar disks remain intact, typically for several Myr. After this time, the planets are largely formed, and the magnetic reconnection region at the inner disk edge is no longer present. Over longer spans of time, however, carbon production can take place on the surfaces of completed planets, or in the interstellar medium. Spallation in the interstellar medium leads to  $[C/O] \sim 10^{-7}$  over a Hubble time [9]. This estimate assumes present-day cosmic ray fluxes, although they could be somewhat larger in the past (since cosmic rays are produced through supernovae, which trace the star formation rate, which was larger in the past). The flux could also be larger in other galaxies in other universes. In any case, the interstellar medium levels of  $[C/O]$  are much smaller than the abundances realized in the reconnection regions of circumstellar disks. Continued irradiation of mature planets leads to similarly low  $[C/O]$  levels, as considered in this section.

After disk dissipation, when planets are fully formed, the host stars continue to generate cosmic radiation near their stellar surfaces, with a reduced particle luminosity. In this context, however, we are interested in small stars, M dwarfs with  $M_* \sim 0.25M_\odot$ , which are observed to have more energetic flaring activity than the Sun. As a result, the expected cosmic ray fluxes from M dwarfs will be significantly larger than solar values during the main sequence phase [58, 59] (but smaller than the fluxes generated at  $r_X$  during the pre-main-sequence phase). More specifically, estimates for the cosmic ray flux from M dwarfs indicate that the cosmic ray flux  $\Phi \sim 10^5 \text{ cm}^{-2} \text{ s}^{-1}$ , for particles with energy  $E > E_0 = 10 \text{ MeV}$  and for a distance  $r = 0.1 \text{ AU}$  from the star [59]. This estimate assumes that the M dwarf continually produces energetic flares (which lead to cosmic ray acceleration) and thus corresponds to the upper end of the possible range. With this flux, the coefficient for the carbon production rate in equation (9) becomes  $\gamma_0 \sim 300 \text{ atoms cm}^{-3} \text{ s}^{-1}$ .

Now consider a planet orbiting a small star at 0.1 AU and assume that it is exposed to cosmic rays over time ( $\Delta t$ ). The planet is likely to be spinning, but at any given time an area  $A \approx \pi R_p^2$  of the planetary surface will be exposed to the flux of energetic particles. The total number of carbon nuclei produced through spallation takes the approximate form

$$N_{C12} \approx (\pi R_p^2) \zeta \gamma_0 (\Delta t) \sim 10^{38} \left( \frac{R_p}{R_\oplus} \right)^2 \left( \frac{(\Delta t)}{10 \text{ Gyr}} \right). \quad (\text{A.1})$$

For comparison, the biosphere of Earth contains 400 – 800 billion tons of carbon, which is equivalent to about  $2 - 4 \times 10^{40}$  carbon atoms. As a result, the number of carbon nuclei that can be produced by spallation over a Hubble time corresponds to less than one percent of the carbon content of our biosphere. With the assumed cosmic ray flux, the star emits a total number of cosmic rays  $N_{CR} \sim 10^{48}$  and the planet intercepts  $N_p \sim 4 \times 10^{40}$  over the time ( $\Delta t$ ), so that  $N_{CR} \gg N_p \gg N_{C12}$ .

The earlier phase of stellar evolution can produce carbon to oxygen ratios up to  $[\text{C/O}] \approx 0.00025$  for  $M_s = 1M_\oplus$  (see Figure 1). Assuming an initial oxygen mass fraction  $X_{O16} = 0.3$ , the total carbon content for an Earth-like planet corresponds to  $N \sim 2 \times 10^{46}$  nuclei. This value far exceeds that total amount of carbon produced through the long term channel of spallation. On the other hand, long term exposure produces carbon at the planetary surface, where it could be more biologically useful.

Looking at these results another way, the number of carbon nuclei produced through long-term enrichment corresponds to the number produced through early enrichment in the upper  $\sim 1$  cm of the planet (in the absence of a planetary magnetic field strong enough to shield the planetary surface from cosmic rays). This thickness is comparable to the scale height for spallation (assuming  $\zeta \sim 1$  cm). As a result, long-term irradiation roughly doubles the carbon content of the upper layer of the planet (1 cm thick).

## References

- [1] M. J. Rees, *Just Six Numbers* (2000, Basic Books)
- [2] J. D. Barrow, *The Constants of Nature: From Alpha to Omega – The Numbers that Encode the Deepest Secrets of the Universe* (2002, Pantheon Books)

- [3] B. J. Carr and M. J. Rees, The Anthropic Principle and the Structure of the Physical World, *Nature* **278** (1979) 611
- [4] J. D. Barrow and F. J. Tipler, *The Anthropic Cosmological Principle* (1986, Oxford Univ. Press)
- [5] C. J. Hogan, Why the Universe is Just So, *Rev. Modern Phys.* **72** (2000) 1149
- [6] M. Tegmark, A. Aguirre, M. J. Rees, and F. Wilczek, Dimensionless constants, cosmology, and other dark matters, *Phys. Rev. D* **73** (2006) 3505
- [7] A. N. Schellekens, Life at the Interface of Particle Physics and String Theory, *Rev. Modern Phys.* **85** (2013) 1491
- [8] J. F. Donoghue, The Multiverse and Particle Physics *Ann. Rev. Nucl. Part. Sci.* **66** (2016) 1
- [9] F. C. Adams, The Degree of Fine-Tuning in our Universe – and Others, *Physics Reports* **807** (2019) 1
- [10] D. D. Clayton, *Principles of Stellar Evolution and Nucleosynthesis* (1983, Univ. Chicago Press)
- [11] R. Kippenhahn and A. Weigert, *Stellar Structure and Evolution* (1990, Springer)
- [12] E. E. Salpeter, Nuclear Reactions in Stars without Hydrogen, *Astrophys. J.* **115** (1952) 326
- [13] F. Hoyle, On Nuclear Reactions Occuring in Very Hot Stars. I. The synthesis of elements from Carbon to Nickel, *Astrophys. J. Suppl.* **1** (1954) 121
- [14] D. N. Dunbar, R. E. Pixley, W. A. Wenzel, and W. Whaling, The 7.68-MeV State in C12, *Phys. Rev.* **92** (1953) 649
- [15] E. Epelbaum, H. Krebs, L. Lähde, D. Lee, and U.-G. Meißner, Dependence of the Triple-alpha Process on the Fundamental Constants of Nature, *Eur. Phys. J. A* **49** (2013) 82

- [16] E. Epelbaum, H. Krebs, D. Lee, and U.-G. Meißner, Ab Initio Calculation of the Hoyle State, *Phys. Rev. Lett.* **106** (2011) 2501
- [17] M. Livio, D. Hollowell, D. M. Truran, and A. Weiss, The Anthropropic Significance of the Existence of an Excited State of C-12, *Nature* **340** (1989) 281
- [18] H. Oberhummer, A. Csótó, and H. Schlattl, Stellar Production Rates of Carbon and its Abundance in the Universe, *Science* **289** (2000) 88
- [19] L. Huang, F. C. Adams, and E. Grohs, Sensitivity of Carbon and Oxygen Yields to the Triple-alpha Resonance in Massive Stars, *Astropart. Phys.* **105** (2019) 13
- [20] F. C. Adams and E. Grohs, Stellar Helium Burning in Other Universes: A Solution to the Triple Alpha Fine-tuning Problem, *Astropart. Phys.* **87** (2017) 40
- [21] P. Ghosh and F. K. Lamb, Disk Accretion by Magnetic Neutron Stars, *Astrophys. J.* **223** (1978) L83
- [22] R. D. Blandford and D. G. Payne, Hydromagnetic Flows from Accretion Disks and the Production of Radio Jets, *Mon. Not. R. Astron. Soc.* **199** (1982) 883
- [23] C. M. Johns-Krull, The Magnetic Fields of Classical T Tauri Stars, *Astrophys. J.* **664** (2007) 975
- [24] F. H. Shu, H. Shang, A. E. Glassgold, and T. Lee, X-rays and Fluctuating X-winds from Protostars, *Science* **277** (1997) 1475
- [25] T. Lee, F. H. Shu, H. Shang, A. E. Glassgold, and K. E. Rehm, Protostellar Cosmic Rays and Extinct Radioactivities in Meteorites, *Astrophys. J.* **506** (1998) 898
- [26] P. Meyer, E. N. Parker, and J. A. Simpson, Solar Cosmic Rays of February 1956 and Their Propagation through Interplanetary Space, *Phys. Rev.* **104** (1956) 768
- [27] M. Padovani, A. Marcowith, P. Hennebelle, and K. Ferrière, Protostars: Forges of cosmic rays? *Astron. Astrophys.* **590** (2016) 8

- [28] E. D. Feigelson, K. Getman, L. Townsley, et al., Global X-Ray Properties of the Orion Nebula Region, *Astrophys. J. Suppl.* **160** (2005) 379
- [29] T. Preibisch, Y.-C. Kim, F. Favata, et al., The Origin of T Tauri X-Ray Emission: New Insights from the Chandra Orion Ultradeep Project, *Astrophys. J. Suppl.* **160** (2005) 401
- [30] D. V. Reames, L. M. Barbier, T. T. Von Rosenvinge, G. M. Mason, J. E. Mazur, and J. R. Dwyer, Energy Spectra of Ions Accelerated in Impulsive and Gradual Solar Events, *Astrophys. J.* **483** (1997) 515
- [31] D. V. Reames, Particle Acceleration at the Sun and in the Heliosphere, *Space Sci. Rev.* **90** (1999) 413
- [32] M.A.I. Van Hollebeke, L. S. Ma Sung, and F. B. McDonald, The Variation of Solar Proton Energy Spectra and Size Distribution with Heliolongitude, *Solar Phys.* **41** (1975) 189
- [33] J. Drazkowska, Y. Alibert, and B. Moore, Close-in Planetesimal Formation by Pile-up of Drifting Pebbles, *Astron. Astrophys.* **594** (2016) 105
- [34] P. Goldreich and W. R. Ward, The Formation of Planetesimals, *Astrophys. J.* **183** (1973) 1051
- [35] B. T. Draine, Interstellar Dust Grains, *Ann. Rev. Astron. Astrophys.* **41** (2003) 241
- [36] K. Lodders and B. Fegley, *The Planetary Scientist's Companion* (1998, Oxford Univ. Press)
- [37] R. Silberberg and C. H. Tsao, Spallation Processes and Nuclear Interaction Products of Cosmic Rays, *Physics Reports* **191** (1990) 351
- [38] N. Soppera, E. Dupont, and M. Bossant, JANIS Book of Proton-Induced Cross-Sections: Comparison of evaluated and experimental data from ENDF/B-VII.1, JENDL/HE-2007, PADF-2007, TENDL-2011 and EXFOR, OECD NEA Data Bank (2012)
- [39] P. Dyer, D. Bodansky, A. G. Seamster, E. B. Norman, and D. R. Maxson, Cross Sections Relevant to Gamma-ray Astronomy: Proton Induced Reactions, *Phys. Rev. C* **23** (1981) 1865

- [40] F. L. Lang, C. W. Werntz, C. J. Crannell, J. I. Trombka, and C. C. Chang, Cross Sections for Production of the 15.10MeV and Other Astrophysically Significant Gamma-ray Lines through Excitation and Spallation of  $^{12}\text{C}$  and  $^{16}\text{O}$  with Protons, *Phys. Rev. C* **35** (1987) 1214
- [41] A. V. Nero and A. J. Howard,  $^{16}\text{O}(p, \alpha)^{13}\text{N}$  Cross Section Measurements, *Nuclear Physics A* **210** (1973) 60
- [42] J. Hernández, L. Hartmann, T. Megeath et al., A Spitzer Space Telescope Study of Disks in the Young  $\sigma$  Orionis Cluster, *Astrophys. J.* **662** (2007) 1067
- [43] A. Johansen, T. Ronnet, M. Bizzarro, M. Schiller, M. Lambrechts, A. Nordlund, and H. Lammer, A Pebble Accretion Model for the Formation of the Terrestrial Planets in the Solar System, *Science Advances* **17** (2021) 0444
- [44] I. Leya, A. N. Halliday, and R. Weiler, Predictable Collateral Consequences of Nucleosynthesis by Spallation Reactions in the Early Solar System, *Astrophys. J.* **594** (2003) 605
- [45] R. C. Reedy and J. R. Arnold, Interaction of Solar and Galactic Cosmic-ray Particles with the Moon, *J. Geophys. Res.* **77** (1972) 537
- [46] A. A. Pavlov, A. K. Pavlov, V. M. Ostryakov, G. I. Vasilyev, P. Mahaffy, and A. Steele, Alteration of the Carbon and Nitrogen Isotopic Composition in the Martian Surface Rocks due to Cosmic Ray Exposure, *J. Geophys. Res.* **119** (2014) 1390
- [47] N. Grevesse and A. J. Sauval, Standard Solar Composition, *Space Sci. Rev.* **85** (1998) 161
- [48] F. C. Adams, Radioactive Planet Formation, *Astrophys. J.*, **919** (2021) 10
- [49] C. Allégre, G. Manhés, and E. Lewin, Chemical Composition of the Earth and the Volatility Control on Planetary Genetics, *Earth Plan. Sci. Lett.* **185** (2001) 49
- [50] B. Marty, The Origins and Concentrations of Water, Carbon, Nitrogen and Noble Gases on Earth, *Earth Planet. Sci. Lett.* **313** (2012) 56

- [51] B. Marty, Origins and Early Evolution of the Atmosphere and the Oceans, *Geochem. Perspect.* **9** (2020) 135
- [52] W.G.R. Miller, J. Maclennan, O. Shorttle, G. A. Gaetani, V. Le Roux, and F. Klein, Estimating the Carbon Content of the Deep Mantle with Icelandic Melt Inclusions, *Earth Plan. Sci. Letters* **523** (2019) 115699
- [53] CRC, Abundance of Elements in the Earth's Crust and the Sea, *Handbook of Chemistry and Physics* 97th Edition (2017) p. 14
- [54] W. F. McDonough, Compositional Models for the Earth's Core, in *Treatise on Geochemistry*, 2nd edition, p. 547 (2003, Elsevier Ltd)
- [55] W. J. Borucki, D. Koch, G. Basri et al., Kepler Planet-Detection Mission: Introduction and First Results, *Science* **327** (2010) 977
- [56] H. Chen, Z. Zhan, A. Youngblood, E. T. Wolf, A. D. Feinstein, and D. E. Horton, Persistence of Flare-driven Atmospheric Chemistry on Rocky Habitable Zone Worlds, *Nature Astron.* **5** (2021) 298
- [57] S. A. Desch, M. A. Morris, H. C. Connolly, and A. P. Boss, A Critical Examination of the X-wind Model for Chondrule and Calcium-rich, Aluminum-rich Inclusion Formation and Radionuclide Production, *Astrophys. J.* **725** (2010) 692
- [58] F. Tabataba-Vakili, J. L. Grenfell, J.-M. Grießmeier, and H. Rauer, Atmospheric Effects of Stellar Cosmic Rays on Earth-like Exoplanets Orbiting M-dwarfs, *Astron. Astrophys.* **585** (2015) 96
- [59] J. M. Grießmeier, F. Tabataba-Vakili, A. Stadelmann, J. L. Grenfell, and D. Atri, Galactic Cosmic Rays on Extrasolar Earth-like Planets. I. Cosmic ray flux *Astron. Astrophys.* **581** (2015) 44